

Supporting Information

1. Structural parameters and mechanical properties	2
2. Strain energy	8
3. Density of states.....	9
4. Electrostatic map.....	10
5. X-ray powder diffraction (XRD) simulations.....	11
6. Born-Oppenheimer Molecular Dynamics – SCC-DFTB calculations	12

1. Structural parameters and mechanical properties.

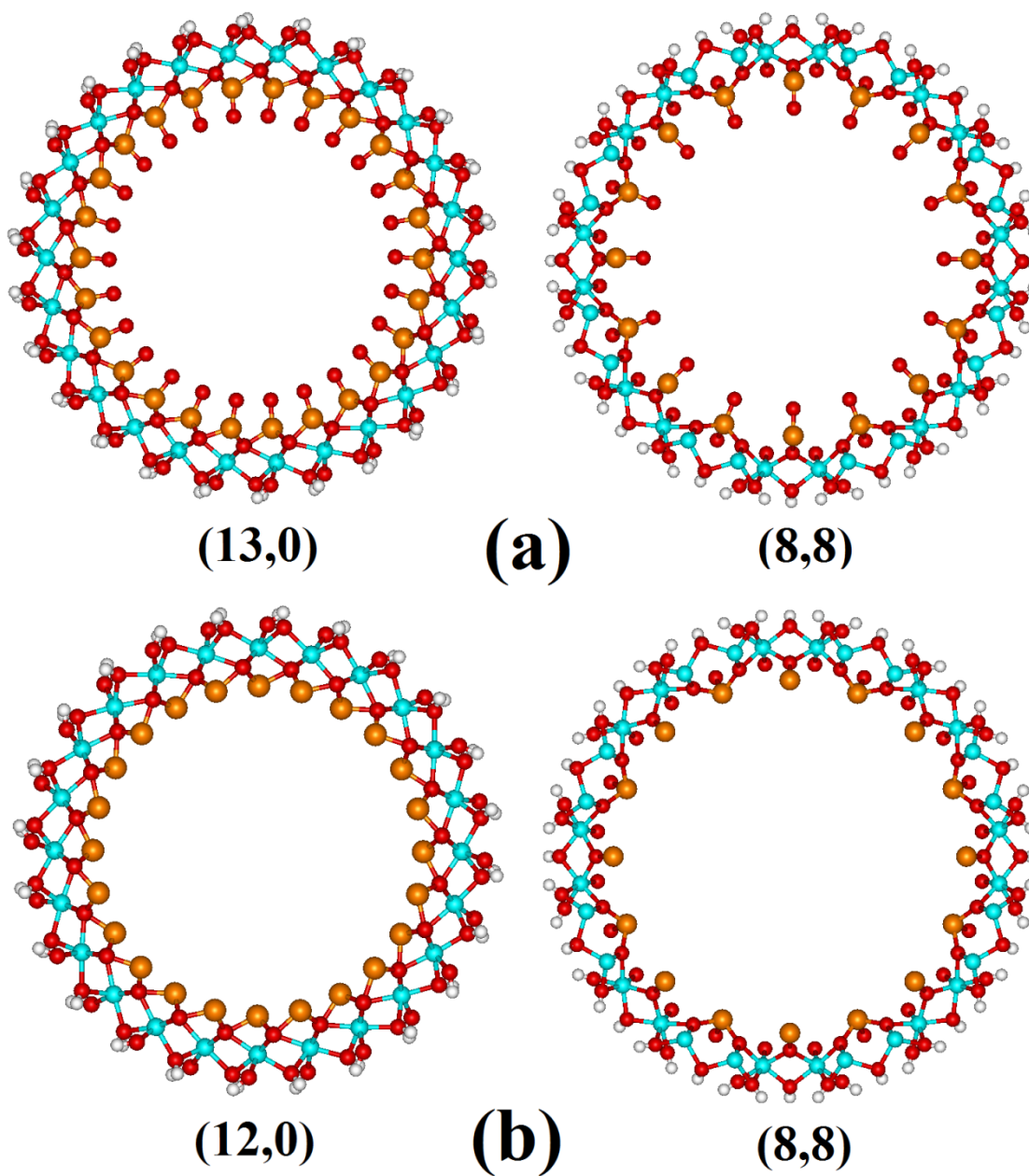


Figure S1 – (a) (13,0) and (8,8) aluminophosphate and (b) (12,0) and (8,8) aluminophosphate nanotubes.

Table S1 – Structural, electronic and elastic properties of aluminophosphate nanotubes

Nanotube	R_{ext} /Å	BG /eV	Y /GPa
(9,0)	8.90	10.1	364
(10,0)	9.66	10.0	362
(11,0)	10.44	10.0	360
(12,0)	11.21	10.0	358
(13,0)	11.99	9.9	357
(14,0)	12.77	9.9	356
(15,0)	13.55	9.9	356
(16,0)	14.33	9.9	355
(17,0)	15.11	9.9	354
(18,0)	15.89	9.9	353
(19,0)	16.67	9.9	352
---	---	---	---
(6,6)	9.96	10.1	386
(7,7)	11.30	10.0	377
(8,8)	12.65	10.0	369
(9,9)	14.00	10.0	364
(10,10)	15.36	9.9	359
(11,11)	16.71	9.9	356
(12,12)	18.07	9.9	354
(13,13)	19.42	9.9	352
(14,14)	20.78	9.9	350
(15,15)	22.13	9.9	350
---	---	---	---
Infinite Layer	---	9.6	---

R_{ext}: external radii; BG: band gap; Y: Young's moduli.

Table S2 – Structural, electronic and elastic properties of aluminophosphate nanotubes

Nanotube	R_{ext} /Å	BG /eV	Y /GPa
(9,0)	09.19	5.3	393
(10,0)	09.96	5.3	396
(11,0)	10.73	5.3	396
(12,0)	11.50	5.3	396
(13,0)	12.28	5.3	395
(14,0)	13.05	5.3	392
(15,0)	13.83	5.3	392
(16,0)	14.61	5.3	396
(17,0)	15.39	5.2	389
(18,0)	16.17	5.2	388
(19,0)	16.95	5.2	387
---	---	---	---
(6,6)	10.26	5.2	414
(7,7)	11.60	5.2	410
(8,8)	13.33	5.2	331
(9,9)	14.29	5.2	406
(10,10)	15.64	5.2	401
(11,11)	16.99	5.2	397
(12,12)	18.34	5.2	392
(13,13)	19.69	5.2	388
(14,14)	21.05	5.2	397
(15,15)	22.40	5.1	387
---	---	---	---
Infinite Layer	---	5.2	---

R_{ext.}: external radii; BG: band gap; Y: Young's moduli.

Table S3 – Structural, electronic and elastic properties of aluminioarsenate nanotubes

Nanotube	R_{ext} /Å	BG /eV	Y /GPa
(9,0)	9.24	7.3	341
(10,0)	9.99	7.4	341
(11,0)	10.76	7.5	340
(12,0)	11.53	7.5	339
(13,0)	12.29	7.5	339
(14,0)	13.07	7.5	338
(15,0)	13.84	7.5	338
(16,0)	14.61	7.5	337
(17,0)	15.39	7.5	337
(18,0)	16.16	7.5	337
(19,0)	16.94	7.5	337

(6,6)	10.28	7.2	361
(7,7)	11.61	7.3	357
(8,8)	12.95	7.3	352
(9,9)	14.29	7.4	348
(10,10)	15.62	7.4	345
(11,11)	16.97	7.4	343
(12,12)	18.31	7.4	341
(13,13)	19.66	7.4	340
(14,14)	21.00	7.4	339
(15,15)	22.35	7.4	338
---	---	---	---
Infinite Layer	---	7.5	---

R_{ext.}: external radii; BG: band gap; Y: Young's moduli.

Table S4 – Structural, electronic and elastic properties of aluminioarsenite nanotubes

Nanotube	R_{ext} /Å	BG /eV	Y /GPa
(9,0)	9.21	4.9	407
(10,0)	9.97	4.9	409
(11,0)	10.74	4.9	411
(12,0)	11.51	4.9	412
(13,0)	12.29	4.9	413
(14,0)	13.06	4.9	414
(15,0)	13.84	4.9	415
(16,0)	14.62	4.8	415
(17,0)	15.40	4.8	416
(18,0)	16.18	4.8	416
(19,0)	16.96	4.8	417

(6,6)	10.28	4.8	449
(7,7)	11.61	4.8	447
(8,8)	12.96	4.8	443
(9,9)	14.30	4.8	440
(10,10)	15.65	4.8	437
(11,11)	17.01	4.8	434
(12,12)	18.37	4.8	431
(13,13)	19.72	4.8	429
(14,14)	21.07	4.8	427
(15,15)	22.43	4.8	426
---	---	---	---
Infinite Layer	---	4.7	---

R_{ext}: external radii; BG: band gap; Y: Young's moduli.

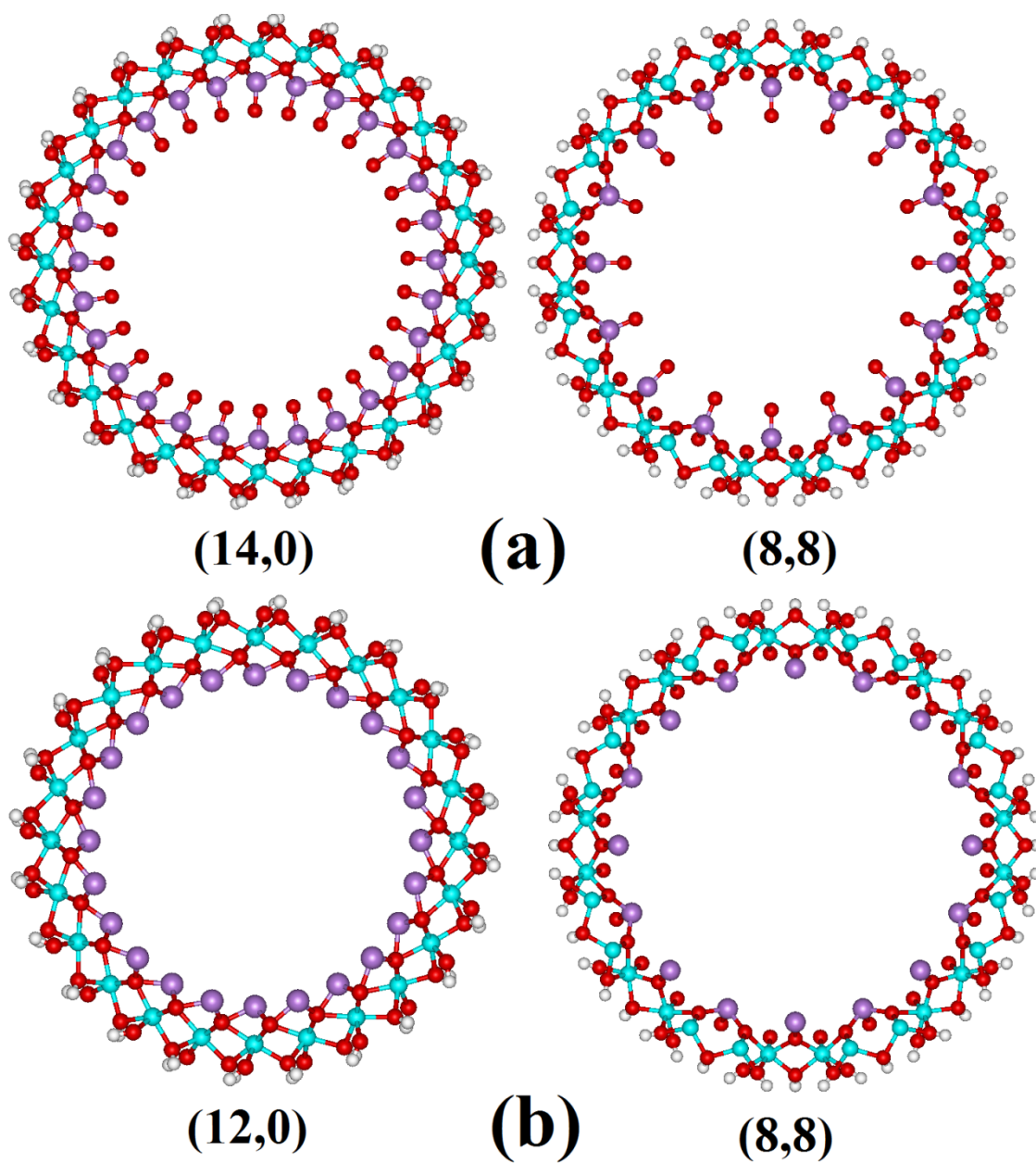


Figure S2 – (a) (14,0) and (8,8) aluminoarsenate and (b) (12,0) and (8,8) aluminoarsenite nanotubes

2. Strain energy

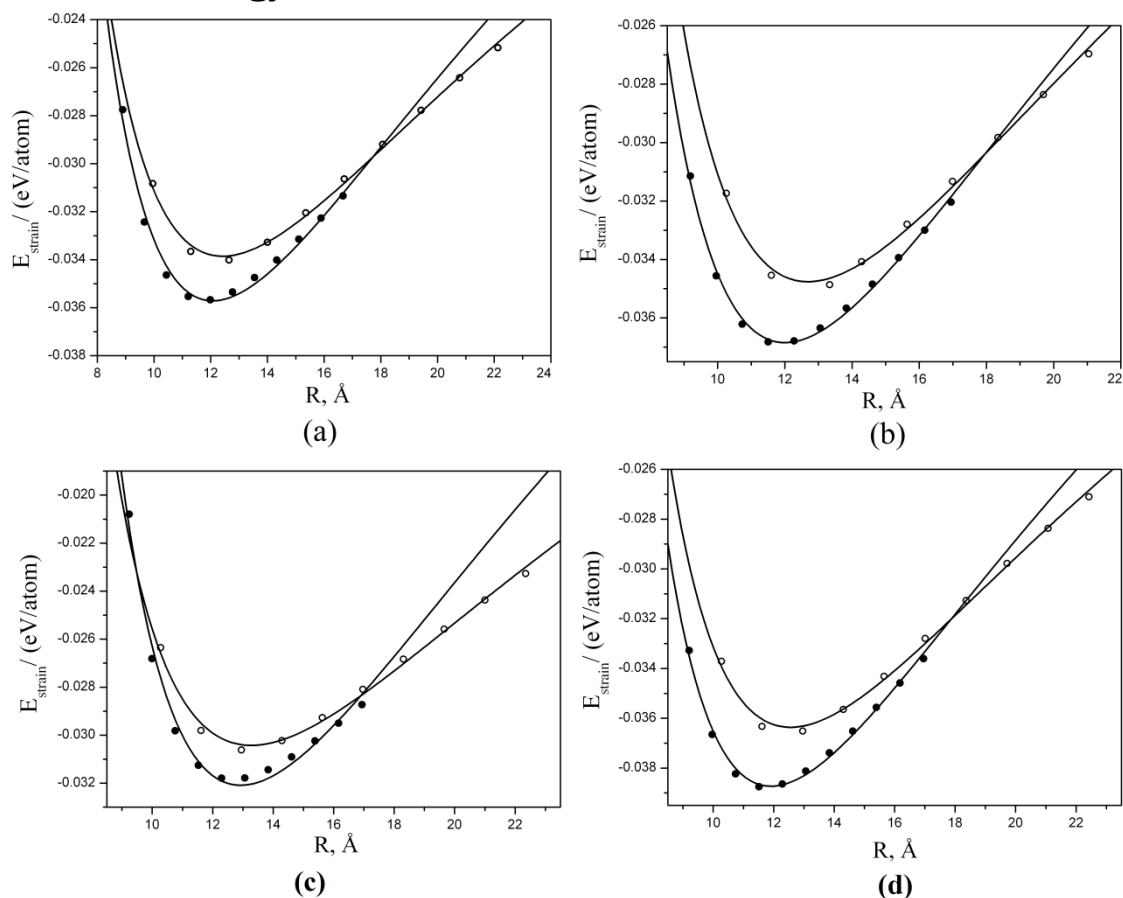


Figure S3 - Strain energy as a function of tube radius for (n,0) (closed circles) and (n,n) (open circles) (a) **imog-P-ate** (Fit values $a = 8.45 \text{ eV}/(\text{atom}\cdot\text{Å}^2)$ and $b = -1.41 \text{ eV}/(\text{atom}\cdot\text{Å})$); (b) **imog-P-ite** (Fit values $a = 11.27 \text{ eV}/(\text{atom}\cdot\text{Å}^2)$ and $b = -1.74 \text{ eV}/(\text{atom}\cdot\text{Å})$); (c) **imog-As-ate** (Fit values $a = 8.61 \text{ eV}/(\text{atom}\cdot\text{Å}^2)$ and $b = -1.43 \text{ eV}/(\text{atom}\cdot\text{Å})$); (d) **imog-As-ite nanotubes** (Fit values $a = 8.57 \text{ eV}/(\text{atom}\cdot\text{Å}^2)$ and $b = -1.28 \text{ eV}/(\text{atom}\cdot\text{Å})$). Results are shown for (9,0)-(19,0) and (6,6)-(15,15) nanotubes.

3. Density of states

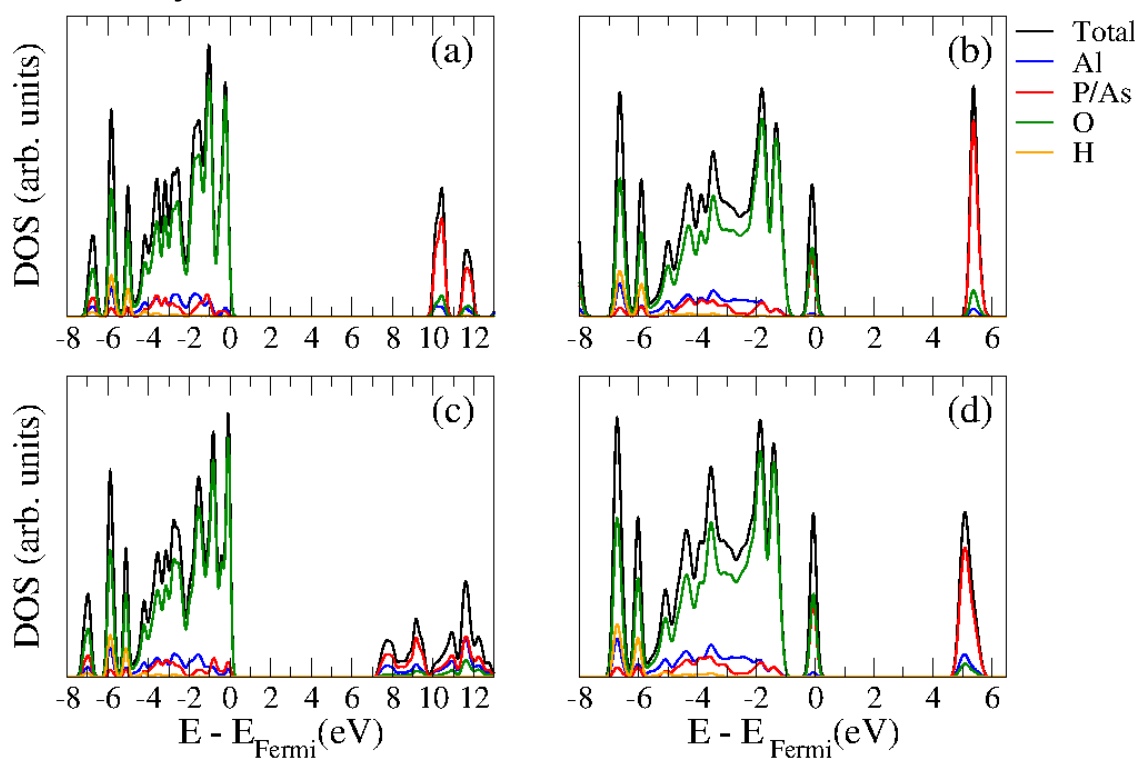


Figure S4 - Total and partial density of states (PDOS) of the *zigzag* (a) imog-P-ate; (b) imog-P-ite; (c) imog-As-ate; (d) imog-As-ite nanotubes. Color of lines: black, total DOS; orange, PDOS of H; blue, PDOS of Al; green, PDOS of O; red, PDOS of P or As. The Gaussians σ value used to obtain the DOS and PDOS was 0.1eV.

4. Electrostatic map.

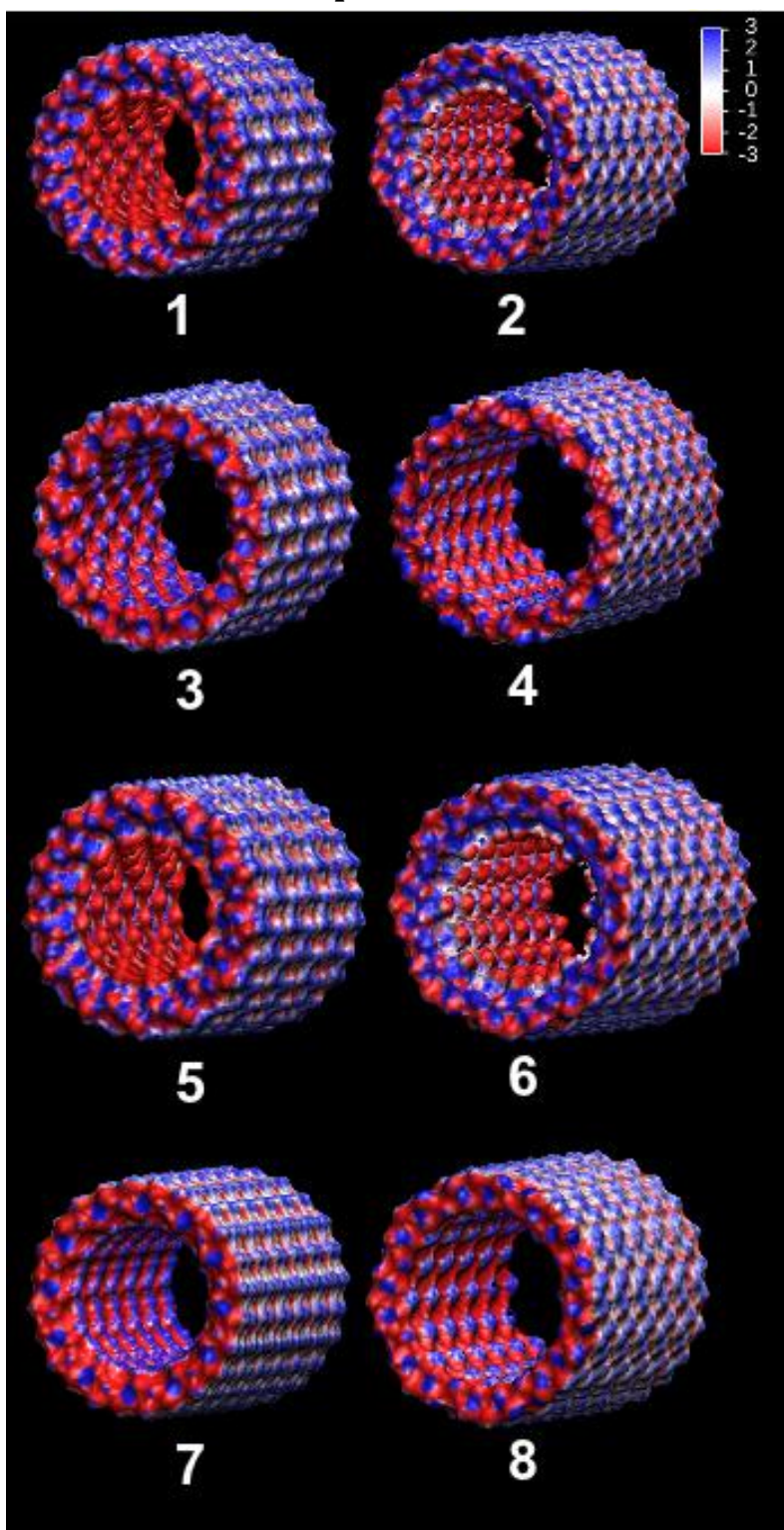


Figure S5 - Electrostatic field of different chiralities of the imogolite-like based nanotubes: (1) (13,0) *zigzag* and (2) (8,8) *armchair* aluminophosphate NTs; (3) (12,0) *zigzag* and (4) (8,8) *armchair* aluminophosphate NTs; (5) (14,0) *zigzag* and (6) (8,8) *armchair* aluminophosphate NTs; (7) (12,0) *zigzag* and (8) (8,8) *armchair* aluminophosphate NTs. Different colors show equipotential surfaces: -3.0, -2.0, -1.0, 1.0, 2.0, 3.0 (25.85 mV).

5. X-ray powder diffraction (XRD) simulations

X-ray powder diffraction (XRD) simulations were carried out using the Mercury program^{1,2}. All diffractograms were calculated with the diffraction angle 2θ assuming values between 10 up to 70 degrees. The X-ray wavelength λ used in this simulation was equal to 1.542 Å as for the copper filtered CuK α radiation. XRD simulations were evaluated using different bundle configurations involving two values of the angle γ between the cell parameters a and b . These angles correspond to a hexagonal ($\gamma = 60$ degrees) and tetragonal ($\gamma = 90$ degrees) intertubular packings. The intertubular distance (lattice parameter $a = b$) used to simulate the XRD of different NT sizes was 24.54 Å for the imogolite (11,0), 27.52 Å for the imog-P-ate (13,0), 26,00 Å for the imog-P-ite (12,0), 29,14 Å for imog-As-ate (14,0) and 26.03 Å for imog-As-ite (12,0) NTs. These values correspond to the distance between the external tubes surface of about 3.0 Å.

1. Bruno, I. J.; Cole, J. C.; Edgington, P. R.; Kessler, M.; Macrae, C. F.; McCabe, P.; Pearson, J.; Taylor, R. Acta Crystallographica Section B 2002, 58, 389-397.
2. Macrae, C. F.; Edgington, P. R.; McCabe, P.; Pidcock, E.; Shields, G. P.; Taylor, R.; Towler, M.; van de Streek, J. Journal of Applied Crystallography 2006, 39, 453-457.

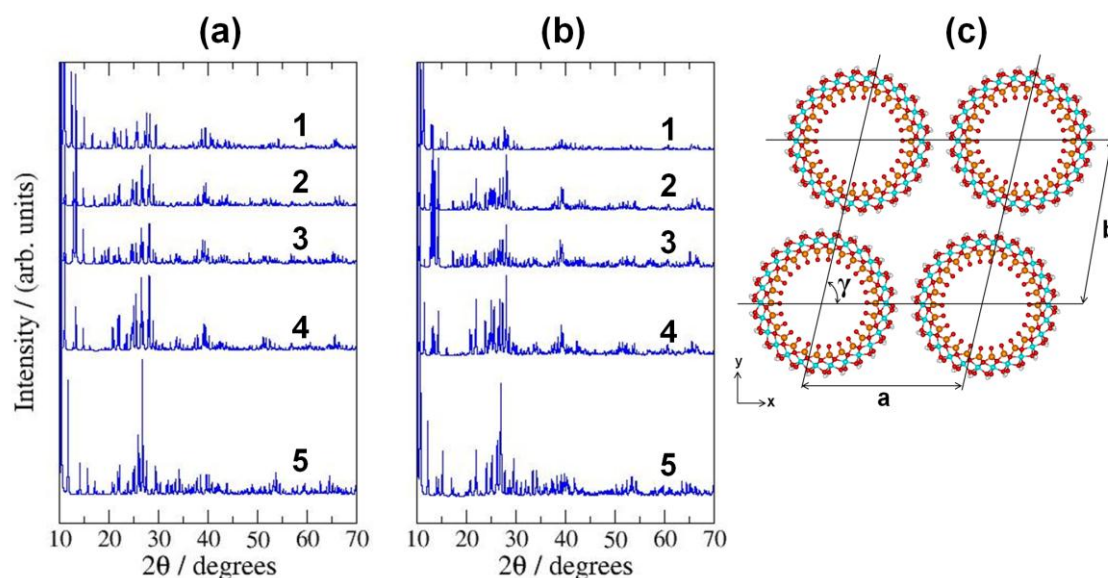


Figure S6 - Experimental and simulated XRD of imogolite-like nanotubes. The simulations were evaluated using the follow set of γ angle (in degrees): (a) $\gamma = 60$ and (b) $\gamma = 90$ degrees. The XRD curves are (1) (11,0) imogolite; (2) (13,0) imog-P-ate NT; (3) (12,0) imog-P-ite NT; (4) (14,0) imog-As-ate NT; (5) (12,0)imog-As-ite NT. (c) shows the definition of the lattice parameters a and b , and the angle γ .

6. Born-Oppenheimer Molecular Dynamics- SCC-DFTB calculations

Born-Openheimer Molecular Dynamics (BOMD) – SCC-DFTB calculations have been performed for the four most stable imogolite-like nanotubes. The timestep was set to 0.5 fs and the systems were thermalized at the NVT ensemble at 400 K using the Berendsen thermostat for 10 ps. For a production run of 50 ps, the NVE ensemble was used resulting in an average temperature (\bar{X}_T) of about 400 K and a standard deviation of the total energy ($\sigma(E_{total})$) less than ± 0.07 eV for all imogolite-like-NTs, table S5. Figure S7 presents the results of the kinetic and potential energy during 50 fs of BOMD/SCC-DFTB simulation for all imogolite-like-NTs. All the structures are stable during the 50 ps at 400 K. The animated gif movie showing the change of the structure using snapshots collected every 50 fs is available.

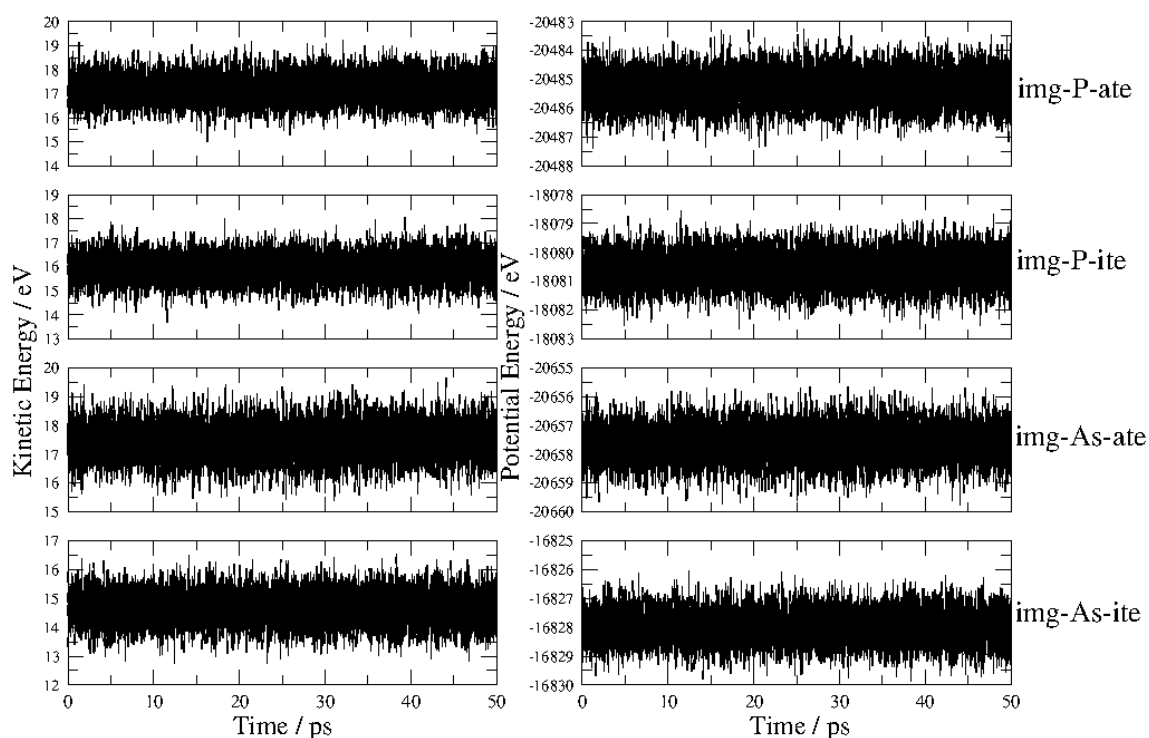


Figure S7 – Variation of kinetic energy and potential energy with respect to the time during the BOMD/SCC-DFTB simulation of aluminophosphate (imog-P-ate), aluminophosphite (imog-P-ite), aluminoarsenate (imog-As-ate) and aluminoarsenite (imog-As-ite) NTs.

Table S5 – The standard deviation of the total energy ($\sigma(E_{total})$) and the average temperature (\bar{X}_T) of the imogolite-like-NTs BOMD/SCC-DFTB simulation using the NVE ensemble during 50 ps.

	$\sigma(E_{total}) / \text{eV}$	\bar{X}_T / K
Imog-P-ate	± 0.05	396
Imog-P-ite	± 0.03	397
Imog-As-ate	± 0.07	400
Imog-As-ite	± 0.03	395